ORGANOMETALLICS

Article

pubs.acs.org/Organometallics

Semibridging Phenyl Ligands in Iridium−Copper and Iridium−Silver Cluster Compounds: Synthesis, Structures, and Bonding

Richard D. Adams,*[,†] Mingwei Chen,[†] Gaya Elpitiya,[†] Xinzheng Yang,*[,‡,§] and Qiang Zhang[†]

[†]Department of Chemistry and Biochemistry, University of South Carolina, Columbia, South Carolina 29208, United States

[‡]Molecular Graphics and Computation Facility, College of Chemistry, University of California, Berkeley, California 94720, United States

[§]State Key Laboratory for Structural Chemistry of Unstable and Stable Species, Institute of Chemistry, Chinese Academy of Sciences, Beijing 100190, People's Republic of China

Supporting Information

ABSTRACT: Reactions of the tetrairidium anion $[Ir_4(CO)_{11}(Ph)]^-$ (**1**) with $[Cu(NCMe)_4][BF_4]$ and $Ag[NO_3]$ have yielded the new iridium−copper and iridium−silver complexes $Ir_4(CO)_{11}(\mu\text{-}\eta^1\text{-Ph})[\mu_3\text{-Cu(NCMe)}]$ (**2**) and $[Et_4N][\{Ir_4(CO)_{11}Ph\}_2(\mu_4\text{-Ag})]$ (**3**), respectively. Compound **2** consists of a tetrahedral Ir_4 cluster with a Cu(NCMe) group bridging one of the Ir_3 triangular faces of the cluster and a semibridging η^1-phenyl ligand that is σ−π-coordinated as a bridge across one of the Ir−Cu bonds. The complex anion of **3** contains two $Ir_4(CO)_{11}Ph$ anions linked by a single quadruply bridging silver atom that has adopted a bow-tie geometry between the four iridium atoms. It contains two terminally coordinated σ-phenyl ligands. Compound **3** reacts with a second equivalent of $Ag[NO_3]$ to yield the uncharged complex $[Ir_4(CO)_{11}]_2(\mu_4\text{-Ag})(\mu\text{-Ag})(\mu_3\text{-Ph})(\mu\text{-Ph})$ (**4**), which contains two $Ir_4(CO)_{11}$ clusters linked by a quadruply bridging silver atom and one triply bridging Ph ligand. The second Ag atom in **4** is an edge bridge on one of the Ir_4 clusters, and the second Ph ligand bridges an Ir−Ag bond to it. When it is dissolved in NCMe, compound **4** is split in two and adds 1 equiv of NCMe to the Ag atom in each half to form the compound $Ir_4(CO)_{11}(\eta^1\text{-Ph})[\mu_3\text{-Ag(NCMe)}]$ (**5**; 73% yield). Unlike **2**, the phenyl ligand in **5** is terminally coordinated. The NCMe ligand is coordinated to the Ag atom. When **4** was treated with PPh_3, the complex $Ir_4(CO)_{11}(\mu\text{-}\eta^1\text{-Ph})[\mu_3\text{-Ag(PPh}_3)]$ (**6**) was obtained in 87% yield. The cluster of **6** is structurally similar to that of **5** except that the phenyl ligand has adopted a semibridging coordination to the silver atom, similar to that found between the phenyl ligand and the copper atom in **2**. All of the new products were characterized by single-crystal X-ray diffraction analyses. The bonding of the bridging phenyl ligands to the clusters in **2** and **4** was analyzed by DFT computational methods.

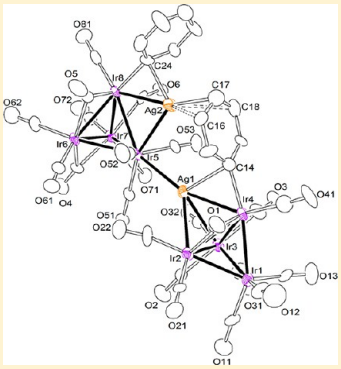

INTRODUCTION

η^1-bridging aryl ligands **A** are commonly found in polynuclear metal complexes of the coinage metals: Cu, Ag, and Au.[1] Aryl copper compounds have been used for a variety of carbon−carbon bond forming cross-coupling reactions.[1a] There are relatively few examples of η^1-bridging aryl ligands in polynuclear transition-metal carbonyl complexes.[2] In most cases, η^1-bridging aryl ligands bridge two similar metal atoms in a symmetrical fashion and the plane of the ring is approximately perpendicular to the metal−metal bond vector (**A**).[1,2] Although they are much less common, η^1-aryl ligands bridging heteronuclear pairs of metal atoms are often coordinated asymmetrically (**B**).[1a,3] In these unsymmetrical cases, the plane of the aryl ring is usually not perpendicular to the M−M′ bond vector. In analogy to the well-known semibridging behavior of carbonyl ligands,[4] we will, hereafter, refer to these asymmetrical bridging phenyl ligands as *semibridging* ligands. Viewed without a charge, all η^1-bridging aryl ligands serve as one-electron donors. η^2-Bridging aryl ligands **C** are also known. These ligands are generally regarded as three-electron donors,[5] and there are still other examples having more extensive interactions of the ring π electrons with neighboring metal atoms.[6]

A **B** **C**

We have recently prepared the tetrairidium anion $[Ir_4(CO)_{11}(Ph)]^-$ (**1**), which contains a terminally coordinated η^1-σ-phenyl ligand by a trans-metalation reaction between $[Ir_4(CO)_{11}Br]^-$ and $SnPh_3(OH)$ or $SnPh_4$ (eq 1).[7]

This anion **1** was found to react with $Ir(CO)(PPh_3)_2Cl$ to yield higher nuclearity iridium cluster complexes[8] and with

Received: February 14, 2013
Published: April 3, 2013

   dx.doi.org/10.1021/om400133w | *Organometallics* 2013, 32, 2416−2426

$[Au(PPh_3)][NO_3]$ and to yield the gold−tetrairidium complex $Ir_4(CO)_{11}(Ph)(\mu\text{-}AuPPh_3)$, which contains a terminally coordinated σ-phenyl ligand (see Scheme 1; the terminally coordinated

Scheme 1

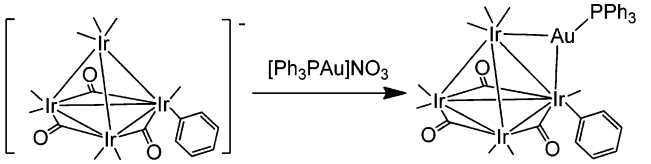

1 $Ir_4(CO)_{11}(Ph)(\mu\text{-}AuPPh_3)$

CO ligands are indicated only by lines to the Ir atoms in our schemes).[9,10]

Iridium is well-known for its ability to produce highly active homogeneous[11] and heterogeneous[12] catalysts. Recently, gold nanoparticles have been shown to exhibit significant activity for the catalytic oxidation of CO and for the oxidation and transformations of unsaturated hydrocarbons.[13] Certain bimetallic catalysts composed of gold and selected transition metals have been shown to exhibit activity even higher than that of pure gold for alcohol and hydrocarbon oxidations and for the synthesis of hydrogen peroxide.[14] A recent report shows that an Ir(III)−Au(I) complex exhibits better catalytic activity for the transfer hydrogenation of nitrobenzene than the corresponding pure iridium and pure gold complexes.[15]

Interest in heterometallic transition-metal cluster complexes containing copper, silver, and gold continues to grow.[16] Nanocrystalline forms of copper and silver have been used as catalysts for the selective oxidation of alcohols.[17] We have now investigated the reactions of anion **1** with $[Cu(NCMe)_4][BF_4]$ and $Ag[NO_3]$ and have obtained the tetrairidium−copper complex $Ir_4(CO)_{11}(\mu\text{-}\eta^1\text{-}Ph)[\mu_3\text{-}Cu(NCMe)]$ (**2**) and a series of iridium−silver complexes: $[Et_4N][Ir_4(CO)_{11}Ph]_2(\mu_4\text{-}Ag)$ (**3**), $[Ir_4(CO)_{11}]_2(\mu_4\text{-}Ag)(\mu\text{-}Ag)(\mu_3\text{-}Ph)(\mu\text{-}Ph)$ (**4**), $Ir_4(CO)_{11}(\eta^1\text{-}Ph)[\mu_3\text{-}Ag(NCMe)]$ (**5**), and $Ir_4(CO)_{11}(\mu\text{-}\eta^1\text{-}Ph)[\mu_3\text{-}Ag(PPh_3)]$ (**6**). Complexes **2**, **4**, and **6** contain unusual σ−π-coordinated, semibridging η^1-phenyl ligands. Two of them, **3** and **4**, contain two tetrairidium clusters linked by bridging silver atoms. The bonding of the σ−π-coordinated phenyl ligands in **2** and **4** were investigated by density functional theory (DFT) molecular orbital calculations. These results are reported herein.

EXPERIMENTAL SECTION

General Data. Reagent grade solvents were dried by the standard procedures and were freshly distilled under nitrogen prior to use. Infrared spectra were recorded on a Thermo Nicolet Avatar 360 FT-IR spectrophotometer. ^{1}H NMR spectra were recorded on a Varian Mercury 300 spectrometer operating at 300.1 MHz. Mass spectrometric (MS) measurements were performed by a direct-exposure probe using electron impact ionization (EI) or by electrospray ionization (ESI) by using a VG 70S instrument. $Ag[NO_3]$ and $[Cu(NCMe)_4][BF_4]$ were obtained from SIGMA-Aldrich and were used without further purification. $[NEt_4][Ir_4(CO)_{11}Ph]$ was prepared according to the published procedure.[6] Product separations were performed by TLC in air on Analtech 0.25 and 0.5 mm silica gel 60 Å F_{254} glass plates. Elemental analyses were performed by Atlantic Microlab, Norcross, GA.

Synthesis of $Ir_4(CO)_{11}(\mu\text{-}\eta^1\text{-}Ph)[\mu_3\text{-}Cu(NCMe)]$ (2). A 6.0 mg portion (0.019 mmol) of $[Cu(NCMe)_4][BF_4]$ was added to 12.0 mg (0.009 mmol) of $[NEt_4][Ir_4(CO)_{11}Ph]$ that was dissolved in 15 mL of CH_2Cl_2. The reaction solution turned red immediately when $[Cu(NCMe)_4][BF_4]$ was added, and the solution was stirred at 25 °C for 30 min. The solvent was then removed in vacuo, and the product was isolated by TLC with a 3/1 hexane/methylene chloride solvent mixture as eluent. This gave 9.0 mg of red $Ir_4(CO)_{11}(\mu\text{-}\eta^1\text{-}Ph)[\mu_3\text{-}Cu(NCMe)]$ (**2**; 77% yield). Spectral data for **2**: IR ν_{CO} (cm^{-1} in CH_2Cl_2) 2082(s), 2044 (vs), 2024 (s), 2006 (s), 1855 (m), 1824 (m); ^{1}H NMR ($CDCl_3$, in ppm) δ 7.542 (d, 2H, $^3J_{H-H}$ = 6.6 Hz, ortho-H of Ph), 6.911−6.988 (m, 3H, meta- and para-H of Ph), 1.84 (s, 3H, NCMe). MS ES (negative ion) for **2**: m/z 1263 ((M + formate)$^-$). The isotope distribution pattern is consistent with the presence of four iridium atoms and one copper atom.

Synthesis of $[NEt_4][\{Ir_4(CO)_{11}Ph\}_2(\mu_4\text{-}Ag)]$ (3). A 6.5 mg portion (0.038 mmol) of $AgNO_3$ was added to 20.0 mg (0.016 mmol) of $[NEt_4][Ir_4(CO)_{11}Ph]$ that was dissolved in 15 mL of CH_2Cl_2. The reaction solution was stirred at 25 °C for 1 h. The solvent was then removed in vacuo, and the product was isolated by TLC with a 1/1 hexane/methylene chloride solvent mixture as eluent. This gave 12.7 mg of yellow $[NEt_4][\{Ir_4(CO)_{11}Ph\}_2(\mu_4\text{-}Ag)]$ (**3**; 64% yield). Spectral data for **3**: IR ν_{CO} (cm^{-1} in CH_2Cl_2) 2078 (m), 2050 (vs), 2009 (s), 1844 (m), 1820 (m); ^{1}H NMR ($CDCl_3$, in ppm) δ 6.62−6.92 (m, 10H, σ-Ph), 3.10 (q, $^3J_{H-H}$ = 6.9 Hz, 8H, CH_2), 0.85 (t, $^3J_{H-H}$ = 6.9 Hz, 12H, CH_3). MS ES (negative ion): m/z 2416 ($[\{Ir_4(CO)_{11}Ph\}_2(\mu_4\text{-}Ag)]^-$), 2389 ($[\{Ir_4(CO)_{11}Ph\}_2(\mu_4\text{-}Ag)]^- - CO$). The isotope distribution pattern is consistent with the presence of eight iridium atoms and one silver atom.

Synthesis of $[Ir_4(CO)_{11}]_2(\mu_4\text{-}Ag)(\mu\text{-}Ag)(\mu_3\text{-}Ph)(\mu\text{-}Ph)$ (4). An 11.0 mg portion (0.004 mmol) of **3** was dissolved in 10 mL of CH_2Cl_2. A 2.7 mg portion (0.016 mmol) of $AgNO_3$ was added, and the reaction solution was stirred for 1 h at 25 °C. The solvent was then removed in vacuo, and the product was isolated by passing over a short silica column (4 cm) with a 1/3 hexane/methylene chloride solvent mixture as eluent to give 7.7 mg of yellow $[Ir_4(CO)_{11}]_2(\mu_4\text{-}Ag)(\mu\text{-}Ag)(\mu_3\text{-}Ph)(\mu\text{-}Ph)$ (**4**; 71% yield). Spectral data for **4**: IR ν_{CO} (cm^{-1} in CH_2Cl_2) 2084 (m), 2047 (vs), 2006 (s), 1841 (m), 1821 (m); ^{1}H NMR ($CDCl_3$, in ppm) δ 7.29−7.74 (m, 10H, σ-Ph). MS ES (negative ion) for **4**: m/z 2568 (M + CO_2H^-), 2540 (M − CO + CO_2H^-). The isotope distribution pattern is consistent with the presence of eight iridium atoms and two silver atoms.

Synthesis of 4 from $[Et_4N][Ir_4(CO)_{11}Ph]$ and $AgNO_3$. A 12.0 mg portion (0.009 mmol) of $[Et_4N][Ir_4(CO)_{11}Ph]$ was dissolved in 10 mL of CH_2Cl_2. A 10.0 mg portion (0.059 mmol) of $Ag[NO_3]$ was added, and the reaction solution was stirred for 1 h at 25 °C. The solvent was then removed in vacuo, and the product was isolated through a short silica column (4 cm) with a 1/3 hexane/methylene chloride solvent mixture as eluent to give 9.2 mg of compound **4** (78% yield).

Synthesis of $Ir_4(CO)_{11}(\eta^1\text{-}Ph)[\mu_3\text{-}Ag(NCMe)]$ (5). A 9.8 mg portion (0.004 mmol) of **4** was dissolved in 10 mL of MeCN. The solution was stirred at 25 °C for 1 h. The solvent was then removed in vacuo, and the product was isolated by chromatography over a short silica column (4 cm) with a 1/3 hexane/methylene chloride solvent mixture as eluent. This gave 7.4 mg of yellow $Ir_4(CO)_{11}(\eta^1\text{-}Ph)[\mu_3\text{-}Ag(NCMe)]$ (**5**; 73% yield). Spectral data for **5**: IR ν_{CO} (cm^{-1} in CH_2Cl_2) 2082 (s), 2043 (vs), 2027 (s), 2007 (s), 1841 (m), 1823 (m); ^{1}H NMR (CD_3CN, in ppm) δ 7.338 (d, 2H, $^1J_{H-H}$ = 6.6 Hz, ortho-H of Ph), 6.804−6.848 (m, 3H, meta- and para-H of Ph). Anal. Found (calcd): C, 17.26 (17.50); H, 0.52 (0.61); N, 1.18 (1.07).

Thermolysis of 5. A ca. 4.0 mg portion of **5** was dissolved in 1.0 mL of CD_3CN in an NMR tube, which was then placed in an oil bath at 50 °C for 48 h. After this period, ^{1}H NMR spectra showed the disappearance of the phenyl resonance of **5** and the appearance of a new single resonance at 7.39 ppm, which is due to the formation of benzene. A 1.1 mg amount of $Ir_4(CO)_{12}$ (32% yield) was subsequently isolated from the reaction mixture.

Synthesis of $Ir_4(CO)_{11}(\mu\text{-}\eta^1\text{-}Ph)[\mu_3\text{-}Ag(PPh_3)]$ (6). A 5.0 mg portion (0.019 mmol) of PPh_3 was added to 10.5 mg (0.004 mmol) of **4** that was dissolved in 15 mL of CH_2Cl_2. The reaction solution was stirred for 30 min at 25 °C. The solvent was then removed in vacuo, and the product was isolated by TLC with a 2/1 hexane/methylene chloride solvent mixture as eluent. This gave 9.1 mg of yellow $Ir_4(CO)_{11}(\mu\text{-}\eta^1\text{-}Ph)[\mu_3\text{-}Ag(PPh_3)]$ (**6**; 87% yield). Spectral data for **6**: IR ν_{CO} (cm^{-1} in CH_2Cl_2) 2081 (s), 2042 (vs), 2027 (s), 2001 (s), 1853 (m), 1824 (m); ^{1}H NMR ($CDCl_3$, in ppm) δ 6.31−6.71 (m, 5H, σ-Ph), 6.90−6.95 (m, 15H, PPh_3). Anal. Found (calcd): C, 27.76 (27.56); H, 1.24 (1.31).

dx.doi.org/10.1021/om400133w | Organometallics 2013, 32, 2416−2426

Crystallographic Analyses. Single crystals of **2** (red), **3** (brown), **4** (yellow), and **6** (red) suitable for X-ray diffraction analyses were obtained by slow evaporation of solvent from a hexane/methylene chloride solvent mixture at −25 °C. Single crystals of **5** (orange) suitable for X-ray diffraction analyses were obtained by slow evaporation of solvent from a MeCN/hexane solvent mixture at −25 °C. Each data crystal was glued onto the end of a thin glass fiber. X-ray intensity data were measured by using a Bruker SMART APEX CCD-based diffractometer and Mo Kα radiation (λ = 0.71073 Å). The raw data frames were integrated with the SAINT+ program by using a narrow-frame integration algorithm.[18] Corrections for Lorentz and polarization effects were also applied with SAINT+. An empirical absorption correction based on the multiple measurement of equivalent reflections was applied in each analysis by using the program SADABS. All structures were solved by a combination of direct methods and difference Fourier syntheses and refined by full-matrix least squares on F^2, using the SHELXTL software package.[19] All non-hydrogen atoms were refined with anisotropic displacement parameters. Hydrogen atoms were placed in geometrically idealized positions and included as standard riding atoms during the least-squares refinements. Crystal data, data collection parameters, and results of the analyses are given in Table S1 (Supporting Information). Compounds **2** and **5** both crystallized in the monoclinic crystal system. The space group $P2_1/n$ was uniquely identified by the systematic absences in the intensity data and further confirmed by the successful solutions and refinements of the structures. There are two symmetry-independent molecules in the asymmetric unit in the crystal of **2**. For compound **5** the space group $P2_1$ was uniquely identified by the systematic absences in the intensity data and subsequently confirmed by successful solutions and refinements of the structure. There is one symmetry-independent molecule in the asymmetric unit in the crystal of **5**. Compounds **3**, **4**, and **6** crystallized in the triclinic crystal system. The space group $P\bar{1}$ was assumed for each analysis and was subsequently confirmed by successful solution and refinement of the structure in each case. There is one symmetry-independent molecule in the asymmetric unit in the crystals of **4** and **6**. For compound **3** there is only half of a symmetry-independent molecule in the asymmetric crystal unit.

Computational Details. All geometry optimizations were performed using the DFT module in the Gaussian 09 suite of ab initio programs[20] for the range-separated and dispersion-corrected hybrid density functional ωB97X-D.[21] Relativistic effective core potential (ECP) basis sets ECP10MDF_VTZ, ECP28MDF_VTZ, and ECP60MDF_VTZ were used for Cu,[22] Ag,[22] and Ir,[23] respectively. An all-electron cc-pVDZ basis set was used for H, C, N, and O atoms.[24] The ωB97X-D functional was selected for this study because it contains both long-range exchange and empirical dispersion corrections, which are important for the modeling of structures with weak interactions and localized anionic or strongly electron donating sites.[25] We believe such basis sets (789 basis functions, 2207 primitive Gaussians, and 900 Cartesian basis functions for **2**; 1464 basis functions, 4132 primitive Gaussians, and 1680 Cartesian basis functions for **4**) used in our study are sufficient for accurate DFT calculations. The geometric structures of **2** and **4** were fully optimized as gas phase (C_s symmetry for **4**). Their ground states were confirmed as singlets through comparison with the optimized high-spin analogues. The fragment analysis for compound **2** was performed with the Amsterdam Density Functional (ADF) 2012 suite of programs[26] by using the meta-generalized gradient approximation (meta-GGA) level nonempirical Tao-Perdew-Staroverov-Scuseria (TPSS) functional[27] for the optimized structure of **2**. The relativistically optimized Slater-type valence quadruple-ζ + 4 polarization function (QZ4P) basis set was used for Cu and Ir atoms, and an all-electron double-ζ (DZ) basis set was used for H, C, N, and O atoms in ADF calculations. The topology of electron densities and charge distributions in the optimized structures of complexes **2** and **4** were analyzed using Bader's quantum theory of atoms in molecules (QTAIM)[28] and the AIMAll software package.[29] Wiberg bond indices[30] were obtained using the NBO 5.0 program.[31] Mayer bond indices[32] were obtained using Gaussian 09.

RESULTS AND DISCUSSION

The reaction of the anion $[Ir_4(CO)_{11}(Ph)]^-$ (**1**) with $[Cu(NCMe)_4][BF_4]$ gave the new iridium−copper complex $Ir_4(CO)_{11}(\mu\text{-}\eta^1\text{-Ph})[\mu_3\text{-Cu(NCMe)}]$ (**2**) in 77% yield. Compound **2** was characterized by single-crystal X-ray diffraction analysis. There are two independent molecules of **2** located in the asymmetric crystal unit. Both molecules are structurally similar. An ORTEP diagram of the molecular structure of one of these two molecules is shown in Figure 1. The molecule consists of a tetrahedral Ir_4 cluster with a Cu atom occupying one of the triangular faces. The Ir−Ir bond distances are similar to those found in the anion **1**.[6] The Ir−Ir distances bridged by the Cu atom are slightly longer (Ir2−Ir3 = 2.8077(5) Å, Ir2−Ir4 = 2.7725(5) Å, Ir3−Ir4 = 2.7499(5) Å) than those that are not (Ir1−Ir2 = 2.7482(5) Å, Ir1−Ir3 = 2.7247(5) Å, Ir1−Ir4 = 2.7307(5) Å). The phenyl ligand serves as a semibridge across the Ir2−Cu1 bond. It is strongly σ-bonded to Ir(2) but is also π-bonded to the Cu atom (see below). The Ir−C bond distance, Ir2−C14 = 2.133(9) Å [Ir6−C54 = 2.124(9) Å], is slightly shorter than the Cu−C distance to the bridging phenyl ligand, Cu1−C14 = 2.171(9) Å [Cu2−C54 = 2.201(8) Å]. (The value in brackets is for the second independent molecule in the crystal.) The Ir−C distance to the terminally coordinated σ-phenyl ligand $Ir_4(CO)_{11}(Ph)(\mu\text{-AuPPh}_3)$ is 2.100(7) Å;[8] that in the anion **1** itself is 2.125(13) Å.[6] The Cu−C distances to the bridging phenyl ligands in the complex $Cu_4(\mu\text{-Ph})_4(SMe_2)_2$, 1.997(8), 2.010(6), 2.054(6), and 2.070(6) Å, are typical of those found for these bridging ligands.[33] Cu−C distances to terminal coordinated Ph ligands are similar in length, e.g. 2.020(4) Å, as found in (triphos)CuPh.[34] The phenyl-bridged Ir−Cu bond, Ir2−Cu1 = 2.6628(12) Å [Ir6−Cu2 = 2.6730(12) Å], is slightly shorter than the

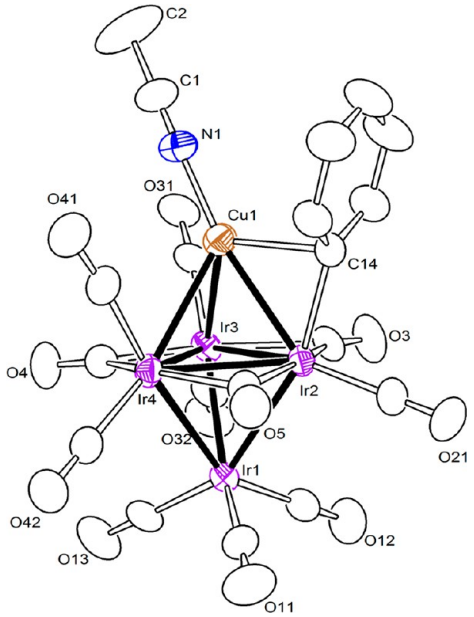

Figure 1. ORTEP diagram of the molecular structure of $Ir_4(CO)_{11}(\mu\text{-}\eta^1\text{-Ph})[\mu_3\text{-Cu(NCMe)}]$ (**2**), showing 30% probability thermal ellipsoids. Selected interatomic bond distances (Å) and angles (deg) for molecule 1 are as follows: Ir1−Ir2 = 2.7482(5), Ir1−Ir3 = 2.7247(5), Ir1−Ir4 = 2.7307(5), Ir2−Ir3 = 2.8077(5), Ir2−Ir4 = 2.7725(5), Ir3−Ir4 = 2.7499(5), Ir2−Cu1 = 2.6628(12), Ir3−Cu1 = 2.7400(13), Ir4−Cu1 = 2.7667(13), Ir2−C14 = 2.133(9), Cu1−C14 = 2.171(9), Cu1−N1 = 1.907(9), C1−N1 = 1.111(13), C1−C2 = 1.474(18); C14−Ir2−Ir1 = 161.7(2), N1− Cu1−Ir2 = 170.0(3).

dx.doi.org/10.1021/om400133w | *Organometallics* 2013, 32, 2416−2426

nonbridged Ir−Cu bonds, Ir3−Cu1 = 2.7400(13) Å and Ir4−Cu1 = 2.7667(13) Å, [Ir7−Cu2 = 2.7232(13) Å and Ir8−Cu2 = 2.7190(15) Å]. The Ir−Cu distances to the triply bridging Cu(NCMe) group in the complex anion $[Ir_6(CO)_{15}Cu(NCMe)]^-$ are similar: 2.646(4), 2.645(4), and 2.617(4) Å.[35] The NCMe ligand lies approximately trans to the Ir(2)−Cu(1) bond: N1− Cu1−Ir2 = 170.0(3)°. Compound **2** contains three bridging carbonyl ligands that circumscribe the Ir_3 triangle that contains the bridging Cu atom. Overall, compound **2** contains a total of 72 valence electrons, so that formally each of the metal atoms can be assigned an 18-electron configuration. Simple electron counting reveals that the uncharged $Ir_4(CO)_{11}[\mu_3$-Cu(NCMe)] fragment has 71 valence electrons. The 72-electron count is completed by the addition of the one electron from the ipso-carbon atom of the uncharged phenyl ring to the Ir atom to form a simple σ bond. To a first approximation, the complex should be stable in this form and there is nothing to be gained by having the phenyl ligand adopt the semibridging coordination mode. Indeed, the structure of compound **5** (see below) has a terminal phenyl ligand. A more detailed account of the bonding of the semibridging phenyl ligand to the metal atoms in **2** was provided by a DFT molecular orbital analysis, which is described below.

When anion **1** was allowed to react with $Ag[NO_3]$, the new iridium−silver complex $[Et_4N][\{Ir_4(CO)_{11}Ph\}_2(\mu_4$-Ag)] (**3**) was obtained in 64% yield. Compound **3** was characterized by single-crystal X-ray diffraction analysis. Compound **3** is a salt consisting of isolated $[Et_4N]$ cations and $[\{Ir_4(CO)_{11}Ph\}_2(\mu_4$-Ag)] anions. An ORTEP diagram of the molecular structure of the complex anion is shown in Figure 2. The molecule consists of

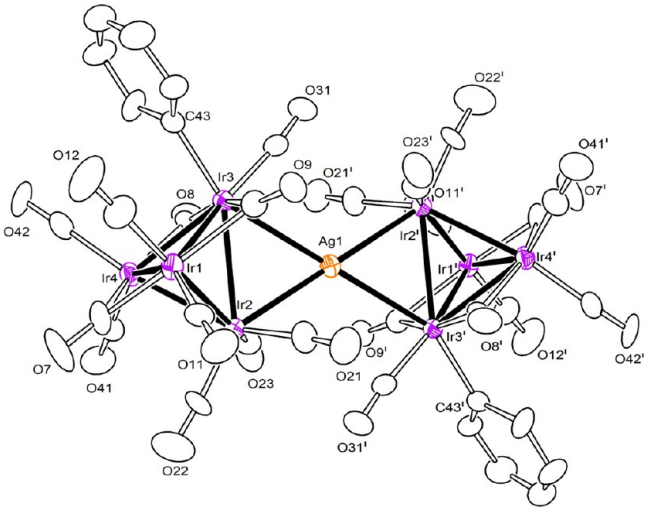

Figure 2. ORTEP diagram of the molecular structure of $[NEt_4]$-$[\{Ir_4(CO)_{11}Ph\}_2(\mu_4$-Ag)] (**3**) showing 30% probability thermal ellipsoids. Selected interatomic bond distances (Å) and angles (deg) of compound **3** are as follows: Ir1−Ir2 = 2.7308(10), Ir1−Ir3 = 2.7449(9), Ir1−Ir4 = 2.7129(10), Ir2−Ir3 = 2.8909(9), Ir2−Ir4 = 2.7369(9), Ir3−Ir4 = 2.7343(9), Ir2−Ag1 = 2.8035(7), Ir3−Ag1 = 3.0060(7), Ir3−C43 = 2.128(18); Ag1−Ir3−C43 = 153.8(5), C43−Ir3−Ir1 = 94.9(5), Ir2−Ag1−Ir3 = 59.563(19), Ag1−Ir3−Ir2 = 56.733(18), Ir2−Ir1−Ir4 = 60.37(3).

two tetrahedral Ir_4 clusters of the anion **1** that are linked by a single quadruply bridging Ag atom. The silver atom lies on a crystallographic center of symmetry in the solid state, so that the two Ir_4 clusters are symmetry related. The silver atom bridges one Ir−Ir bond in each Ir_4 cluster. The four Ir atoms exhibit a planar "bow-tie" geometry about the Ag atom. The planar bow-tie structure for silver is rare among metal carbonyl cluster complexes, but there are two crystallographically characterized examples, both existing in anionic complexes: $[\{Os_3(CO)_{11}H\}_2(\mu_4$-Ag)]$^-$ and $[\{Rh_6(CO)_{15}(C)\}_2(\mu_4$-Ag)]$^{3-}$.[36,37] The Ag-bridged Ir−Ir bond in **3**, Ir2−Ir3 = 2.8909(9) Å, is significantly longer than the other Ir−Ir bonds, which range from 2.7129(10) to 2.7449(9) Å. The latter are very similar to those found in the anion **1**.[6] Each Ir_4 cluster contains one terminally coordinated σ-phenyl ligand that lies approximately trans to one of the Ir−Ag bonds. The Ir−C bond distance is similar to that found in **1**: Ir3−C43 = 2.128(18) Å.[6] The complex anion has an overall charge of 1−; therefore, since each Ir_4 cluster is formally 1−, the Ag atom can be viewed formally as having a 1+ charge. The two independent Ir−Ag bond distances are significantly different in length: Ir2−Ag1 = 2.8035(7) Å and Ir3−Ag1 = 3.0060(7) Å. The Ir3−Ag1 bond that lies approximately trans to the σ-phenyl ligand is the longer of the two. As found in both **1** and **2**, there are three bridging CO ligands about one of the triangular Ir_3 faces, Ir2−Ir3−Ir4.

Compound **3** reacts with a second equivalent of $Ag[NO_3]$ to yield the uncharged complex $[Ir_4(CO)_{11}]_2(\mu_4$-Ag)(μ-Ag)-(μ_3-Ph)(μ-Ph) (**4**) in 71% yield by the addition of a second Ag^+ ion. Compound **4** was also obtained in 78% yield directly by the reaction of **1** with an excess of $Ag[NO_3]$. Compound **4** was characterized by single-crystal X-ray diffraction analysis. An ORTEP diagram of the molecular structure of the complex anion is shown in Figure 3. Compound **4** consists of two tetrahedral Ir_4

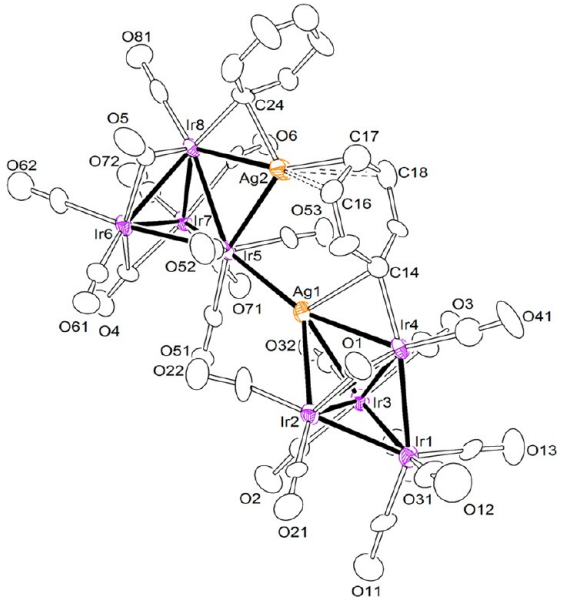

Figure 3. ORTEP diagram of the molecular structure of $[Ir_4(CO)_{11}]_2(\mu_4$-Ag)(μ-Ag)(μ_3-Ph)(μ-Ph) (**4**) showing 30% probability thermal ellipsoids. Selected interatomic bond distances (Å) and angles (deg) of compound **4** are as follows: Ir1−Ir2 = 2.7212(18), Ir1−Ir3 = 2.7125(18), Ir1−Ir4 = 2.7388(19), Ir2−Ir3 = 2.7530(18), Ir2−Ir4 = 2.7828(17), Ir3−Ir4 = 2.8128(16), Ir5−Ir6 = 2.7676(17), Ir5−Ir7 = 2.7701(17), Ir5−Ir8 = 2.8817(18), Ir6−Ir7 = 2.6967(18), Ir6−Ir8 = 2.7176(17), Ir7−Ir8 = 2.7096(16), Ir2−Ag1 = 2.899(3), Ir3−Ag1 = 2.902(3), Ir4−Ag1 = 2.859(3), Ir5−Ag1 = 2.766(3), Ir5−Ag2 = 2.781(3), Ir8−Ag2 = 2.941(3), Ir4−C14 = 2.11(3), Ag1−C14= 2.56(3), Ag2−C16 = 2.74(9), Ag2−C17 = 2.42(4), Ag2−C18 = 2.71(3), Ag2−C24 = 2.27(3), Ir8−C24 = 2.13(3); C14−Ir4−Ir1 = 169.5(8), Ir2−Ir1−Ir4 = 61.28(5), C24−Ir8−Ir6 = 143.8(10), Ag1−Ir5−Ir6 = 146.57(8), Ag2−Ir5 −Ag1 = 83.24(8).

clusters of the anion **1** that are linked by bridging Ag atoms. The silver atom Ag1 is a quadruply bridging atom that is bonded to

dx.doi.org/10.1021/om400133w | *Organometallics* 2013, 32, 2416−2426

three Ir atoms, Ir2−Ir3−Ir4, of one cluster and one Ir atom, Ir5, of the second cluster. The second silver atom, Ag2, is a bridge across the Ir5−Ir8 edge of the second cluster. The two phenyl ligands have adopted semibridging coordinations from Ir atoms to the Ag atoms. The phenyl ring, C14−C19, contains significant interactions with the three metal atoms Ir4, Ag1, and Ag2 and could thus be described as a triply bridging ligand. The ipso carbon atom of this ring is strongly σ^1- bonded to Ir4 (Ir4−C14 = 2.11(3) Å) but is also weakly bonded to Ag1 (Ag1−C14 = 2.56(3) Å). Most interestingly, the para carbon C17 and to a lesser degree the meta carbon atoms of this ring are also bonded to Ag2. The Ag2−C17 distance, 2.42(4) Å, is shorter than the Ag1−C14 distance and implies a fairly strong interaction (see the computational analyses described below). The Ag−C distances to the meta carbon atoms, Ag2−C16 = 2.74(9) Å and Ag2−C18 = 2.71(3) Å, suggest some weak bonding between these atoms. We think this ligand is best described as a 1,4-η^2 triple bridge. Other forms of η^n bridging phenyl ligands have been reported, but the 1,4-η^2 triple bridge found here in compound **4** appears to be unique.[3b,5,6] The second phenyl ligand is a simple η^1 semibridge across the Ir8−Ag2 bond: Ir8−C24 = 2.13(3) Å and Ag2−C24 = 2.27(3) Å.

When compound **4** was dissolved in MeCN, the complex was split in two to yield two $AgIr_4$ clusters and 1 equiv of NCMe was added to each half to give the new complex $Ir_4(CO)_{11}(\eta^1$-Ph)$[\mu_3$-Ag(NCMe)] (**5**) in 73% yield. Compound **5** was characterized by single-crystal X-ray diffraction analysis, and an ORTEP diagram of its molecular structure is shown in Figure 4.

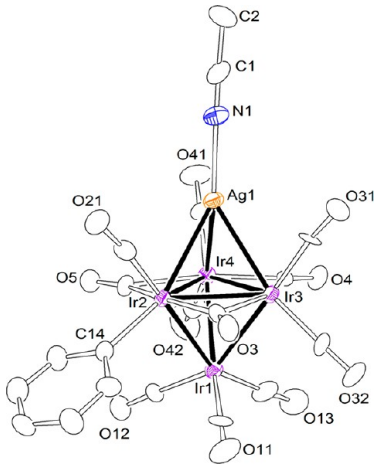

Figure 4. ORTEP diagram of the molecular structure of $Ir_4(CO)_{11}(\eta^1$-Ph)$[\mu_3$-Ag(NCMe)] (**5**) showing 30% probability thermal ellipsoids. Selected interatomic bond distances (Å) and angles (deg) of compound **5** are as follows: Ir1−Ir2 = 2.7264(8), Ir1−Ir3 = 2.7217(7), Ir1−Ir4 = 2.7209(9), Ir2−Ir3 = 2.8141(7), Ir2−Ir4 = 2.8133(6), Ir3−Ir4 = 2.7802(8), Ir2−Ag1 = 2.8711(13), Ir3−Ag1 = 2.8374(10), Ir4−Ag1 = 2.8724(14), Ir2−C14 = 2.102(16), Ag1−N1 = 2.190(12), C1−N1 = 1.102(18); C14−Ir2−Ir1 = 94.9(4), C14−Ir2−Ag1 = 156.4(4), N1−Ag1−Ir2 = 144.0(4).

The molecule consists of a tetrahedral Ir_4 cluster with an Ag(NCMe) group occupying one of the triangular faces of the Ir_4 cluster. In this sense the molecule is similar to that of **2**, but unlike **2**, the phenyl ligand in **5** is not a semibridging ligand. It is instead a terminally coordinated σ-phenyl ligand that lies approximately trans to one of the Ir−Ag bonds, similar to that found for one of the two phenyl ligands in **3**. The Ir−C bond distance, Ir2−C14 = 2.102(16) Å, is similar to that found in **3**. The Ag-bridged Ir−Ir bond distances, Ir2−Ir3 = 2.8141(7) Å, Ir2−Ir4 = 2.8133(6) Å, and Ir3−Ir4 = 2.7802(8) Å, are significantly longer than the unbridged bonds, Ir1−Ir2 = 2.7264(8) Å, Ir1−Ir3 = 2.7217(7) Å, and Ir1−Ir4 = 2.7209(9) Å. The Ir−Ag bond distances, Ir2−Ag1 = 2.8711(13) Å, Ir3−Ag1 = 2.8374(10) Å, and Ir4−Ag1 = 2.8724(14) Å, are similar to those found in **3** and **4**. As found in **2** and **4**, there are three bridging CO ligands about the Ir_3 triangle that supports the triply bridging heterometal atom. The metal cluster in **5** contains a total of 72 valence electrons, which is formally consistent with 18-electron configurations at each of the metal atoms. Interestingly, when it is gently heated (reflux in a CH_2Cl_2 solution), compound **5** did not lose NCMe and reconvert to **4** but was instead transformed into $Ir_4(CO)_{12}$ by loss of the Ag metal atom and the NCMe ligand and the acquisition of a CO ligand. Benzene was also observed to form in this decomposition, apparently derived from the phenyl ligand. The source of the proton needed to create the benzene has not been established.

The reaction of **4** with PPh_3 gave the new complex $Ir_4(CO)_{11}(\mu$-η^1-Ph)$[\mu_3$-Ag$(PPh_3)]$ (**6**) in 87% yield. Compound **6** was characterized by single-crystal X-ray diffraction analysis, and an ORTEP diagram of its molecular structure is shown in Figure 5. The structure of the Ir_4Ag cluster of **6** similar to that of

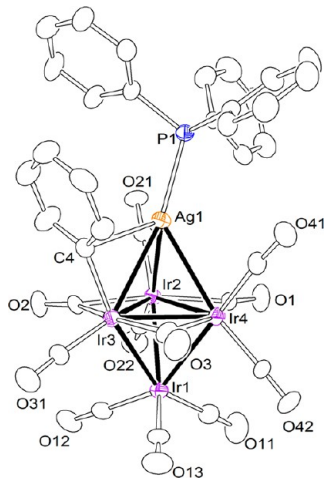

Figure 5. ORTEP diagram of the molecular structure of $Ir_4(CO)_{11}(\mu$-η^1-Ph)$[\mu_3$-Ag$(PPh_3)]$ (**6**) showing 30% probability thermal ellipsoids. Selected interatomic bond distances (Å) and angles (deg) of compound **6** are as follows: Ir1−Ir2 = 2.7282(6), Ir1−Ir3 = 2.7566(6), Ir1−Ir4 = 2.7309(6), Ir2−Ir3 = 2.8017(6), Ir2−Ir4 = 2.7740(6), Ir3−Ir4 = 2.7941(6), Ir2−Ag1 = 2.9263(9), Ir3−Ag1 = 2.9219(9), Ir4−Ag1 = 2.9382(9), Ir3−C4 = 2.144(11), Ag1−C4 = 2.506(10), Ag1−P1 = 2.417(3); C4−Ir3−Ir1 = 167.1(3), Ag1−Ir2−Ir3 = 61.30(2), P1− Ag1−Ir2 = 130.49(7), Ir2−Ir1−Ir4 = 61.080(15).

5, but most interestingly, the phenyl ligand which is terminally coordinated in **5** has adopted a semibridging coordination mode in **6** similar to that observed in **2**: Ir3−C4 = 2.144(11) Å and Ag1−C4 = 2.506(10) Å. We can only conclude that energetically there is not a great difference between the terminal and semibridging coordination modes of the phenyl ligand in these cluster complexes. This is supported by the computational analysis described below. The Ir−Ir distances in **6** are similar to those in **5**, but the Ir−Ag distances are significantly longer than those in **5**,: Ir2−Ag1 = 2.9263(9) Å, Ir3−Ag1 = 2.9219(9) Å, and Ir4−Ag1 = 2.9382(9) Å. The phosphine ligand is coordinated to the silver atom: Ag1−P1 = 2.417(3) Å.

dx.doi.org/10.1021/om400133w | *Organometallics* 2013, 32, 2416−2426

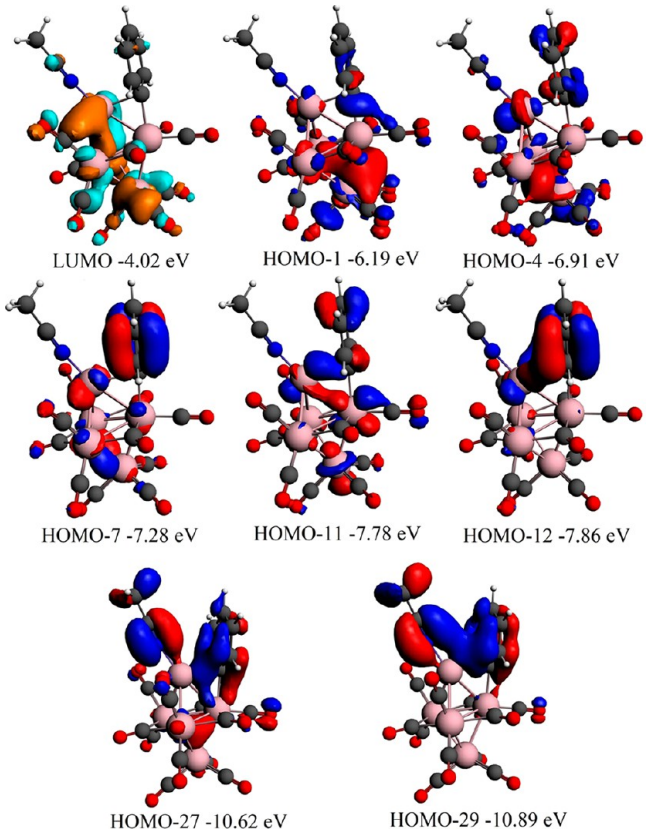

Figure 6. Selected molecular orbitals with calculated energy values showing interactions between the metal atoms and the phenyl ring in **2**.

Computational Analyses of the Bonding in 2 and 4. To understand the nature of the semibridging bonding of the phenyl ligands in **2** and **4** in greater detail, geometry-optimized DFT molecular orbital calculations were performed. Selected MOs that pertain to the bonding of the phenyl ligand across the Ir−Cu bond in **2** are shown in Figure 6. The HOMO-1 shows σ bonding of the ipso carbon atom to the iridium atom. HOMO-4, -7, -11, -12, -27, and -29 all show interactions between π orbitals on the ring with suitably oriented d orbitals on the copper atom. HOMO-11, -12, -27, and -29 are clearly ring to metal bonding in character, while the orbitals HOMO-4 and -7 are weak ring to metal antibonding forms.

An ADF fragment analysis reveals the origin of the MOs in Figure 7. The fragment MOs were created for the phenyl ring (shown on the right-hand side) and the $Ir_4(CO)_{11}[\mu_3\text{-}Cu(NCMe)]$ group (shown on the left-hand side) in the combined MO/energy level diagram shown in Figure 7. HOMO-1 of **2** is the most important orbital for the bonding of the phenyl ring to the metal cluster. The bonding is a combination of the singly occupied MO (SOMO) of the phenyl ring fragment and the singly occupied MO of the $Ir_4(CO)_{11}[\mu_3\text{-}Cu(NCMe)]$ fragment. This orbital serves as the basis for what would commonly be referred to as a phenyl−iridium, C−Ir, σ bond. HOMO-11 shows the existence of phenyl−copper bonding interactions which are derived from HOMO-1 of the phenyl ring fragment and HOMO-6 of the $Ir_4(CO)_{11}[\mu_3\text{-}Cu(NCMe)]$ fragment, but there is also an antisymmetric combination of these two fragment orbitals that manifests itself in HOMO-4. Since both of these orbitals are filled, the phenyl−Cu bonding gained by formation of HOMO-11 is reduced by the interactions in HOMO-4. A similar competing relationship is found between HOMO-12 and -7 in **2**.

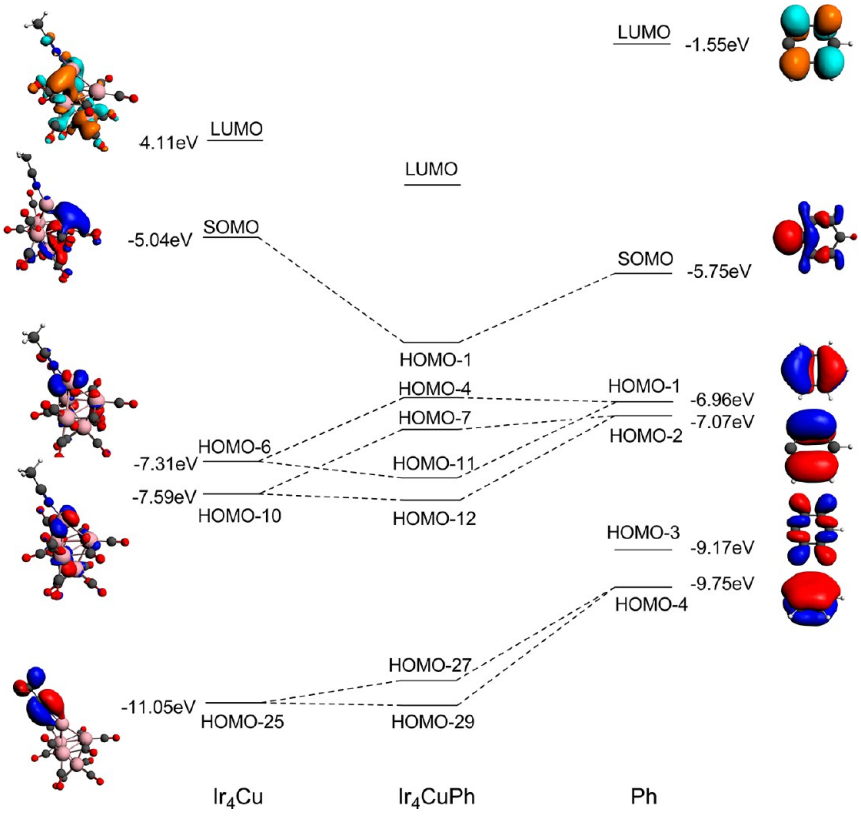

Figure 7. Molecular orbital fragment analysis including an energy level diagram for **2**, showing the metal−phenyl ring interactions.

dx.doi.org/10.1021/om400133w | *Organometallics* 2013, 32, 2416−2426

The Cu−ring orbital interactions in these two MOs are created by symmetric and antisymmetric combinations of the HOMO-2 ring fragment orbital and HOMO-10 of the $Ir_4(CO)_{11}[\mu_3$-Cu(NCMe)] fragment. HOMO-4 of the phenyl ring forms significant interactions with HOMO-25 of the cluster fragment to form HOMO-27 and -29. Our calculations revealed no significant bonding interactions between the metal atoms and the unoccupied π orbitals of the phenyl ring. One reason for this is because the ring π orbitals lie at too high energy: e.g., see the location of the ring lowest unoccupied molecular orbital (LUMO) shown in Figure 7.

The bonding in **2** was further analyzed by calculating the electron densities at the bond critical points (BCPs) in the optimized structure by using the QTAIM method. Selected electron densities at important BCPs are shown in Figure 8. The

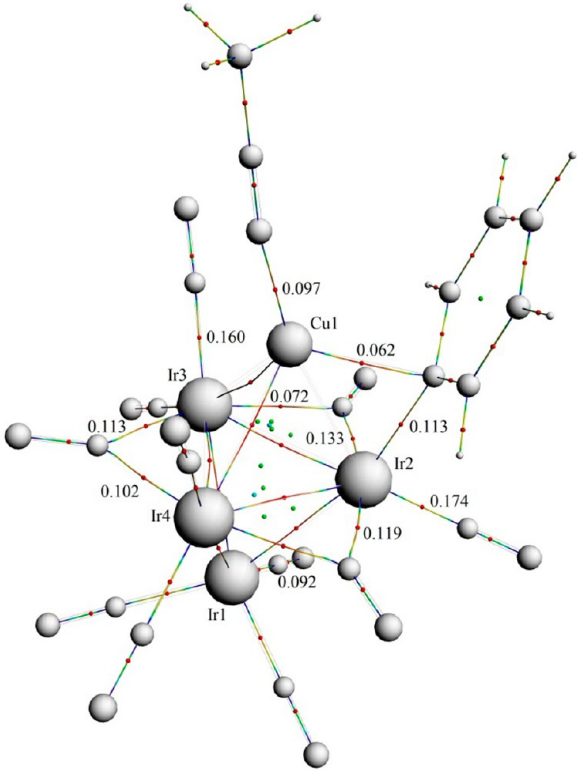

Figure 8. Selected electron densities at bond critical points calculated by QTAIM using the optimized structure of **2**.

electron densities at the BCPs in the C1−Cu and C1−Ir2 bonds are 0.062 and 0.113 e/bohr^3, respectively. Such electron densities indicate that the bond strength between C1 and Cu is about half of the bond strength between C1 and Ir2 and support the description as a semibridging phenyl ligand between Cu and Ir2. The 0.113 e/bohr^3 electron density at the BCP in the C1−Ir2 bond is very similar to the electron densities calculated between Ir atoms and bridging carbonyl ligands in **2** (see Figure 8).

Before discussing the bonding in **4**, it would be appropriate to consider the valence electron count about the metal atoms. First let us consider the stable, related compound $Ir_4(CO)_{11}(Ph)(\mu$-$AuPPh_3)$ (**7**; cf. Scheme 1).[8] Assuming that the phenyl group and $AuPPh_3$ group in **7** each donate one electron to the Ir atoms, then the Ir_4 cluster contains a total of 60 valence electrons and each Ir formally achieves an 18-electron configuration. Compound **4** can be viewed as a combination of two $AgIr_4(CO)_{11}(Ph)$ fragments. Ag is electronically similar to Au. Electronically, the primary difference between **7** and the $AgIr_4(CO)_{11}(Ph)$ fragment is the presence or absence of the PPh_3 ligand which serves as a two-electron donor to the Au atom. In the absence of a PPh_3 ligand or its equivalent, each $AgIr_4(CO)_{11}(Ph)$ fragment is formally electron deficient by the amount of two electrons. Two of those missing electrons in **4** are made up by the formation of the Ir−Ag bond between the atoms Ir(5) and Ag(1) linking the two clusters; thus, compound **4** itself is only deficient by the amount of two electrons. As can be seen in Figure 3, there is an important secondary bonding interaction to one of the semibridging phenyl ligands; in particular, the μ_3-semibridging Ph ligand represented by the ipso carbon atom labeled C14 in Figure 3 is also coordinated by the π electrons in its ring to the atom Ag2. In the absence of this interaction, Ag2 would be the primary site of this electron deficiency.

The DFT optimized structure of **4** with the DFT labeling scheme is shown in Figure 9. Table 1 gives the lengths of some

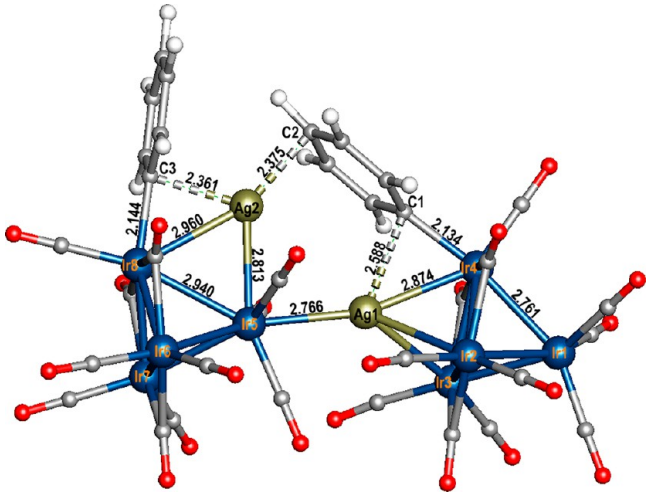

Figure 9. DFT optimized structure of **4**. Bond lengths are given in Å.

Table 1. Comparison of Selected Bond Lengths and Bond Indices of 4

	bond length (Å)		bond index	
bond	calcd	exptl	Wiberg	Mayer
C1−Ag1	2.588	2.557	0.0713	0.0896
C1−Ir4	2.134	2.105	0.4339	0.8846
C2−Ag2	2.375	2.429	0.0777	0.2456
C3−Ag2	2.361	2.262	0.1072	0.2765
C3−Ir8	2.144	2.134	0.4418	0.7324
Ag1−Ir4	2.874	2.858	0.0610	0.1214
Ag1−Ir5	2.766	2.766	0.0738	−0.5082
Ag2−Ir5	2.813	2.781	0.1068	−0.0262
Ag2−Ir8	2.960	2.941	0.0487	0.0248
Ir5−Ir8	2.940	2.882	0.1606	−0.0529
Ir1−Ir4	2.761	2.739	0.2198	0.5353

important bonds obtained from DFT optimization and their Wiberg bond indices obtained from NBO analysis. The experimental bond lengths are also listed for comparison. The optimized C1−Ag1, C1−Ir4, C2−Ag2, C3−Ag2, and C3−Ir8 distances are 2.588, 2.134, 2.375, 2.361, and 2.144 Å, respectively, which are virtually the same as the experimental values. Such small differences validate that the ωB97X-D functional and corresponding basis sets are appropriate for the study of the structure and bonding properties of this complex.

dx.doi.org/10.1021/om400133w | *Organometallics* 2013, 32, 2416−2426

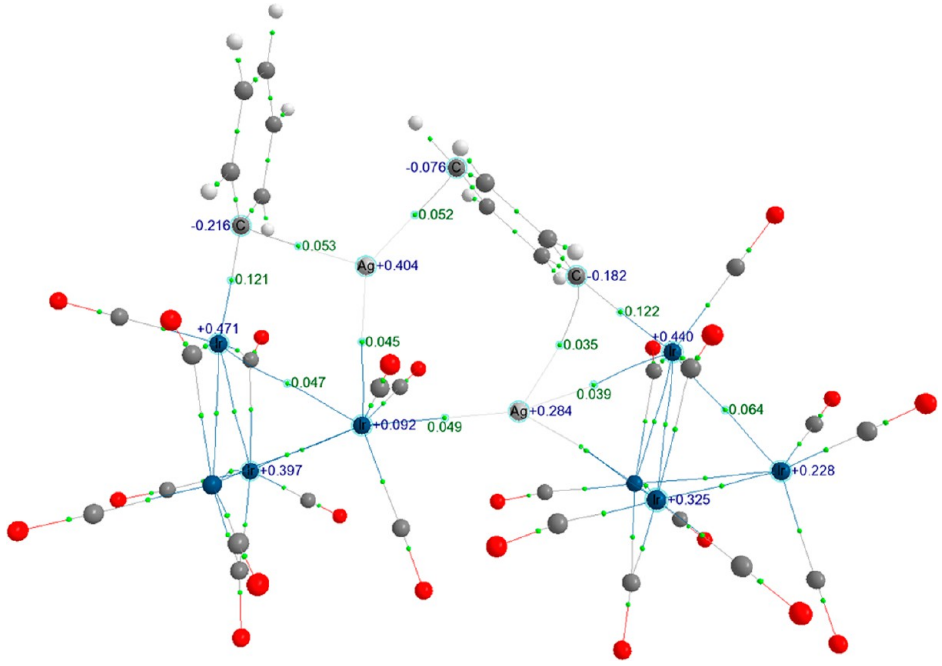

Figure 10. QTAIM analysis of bond paths with electron densities at selected bond critical points (green) and atomic charges (blue) in the optimized structure of **4**.

Scheme 2

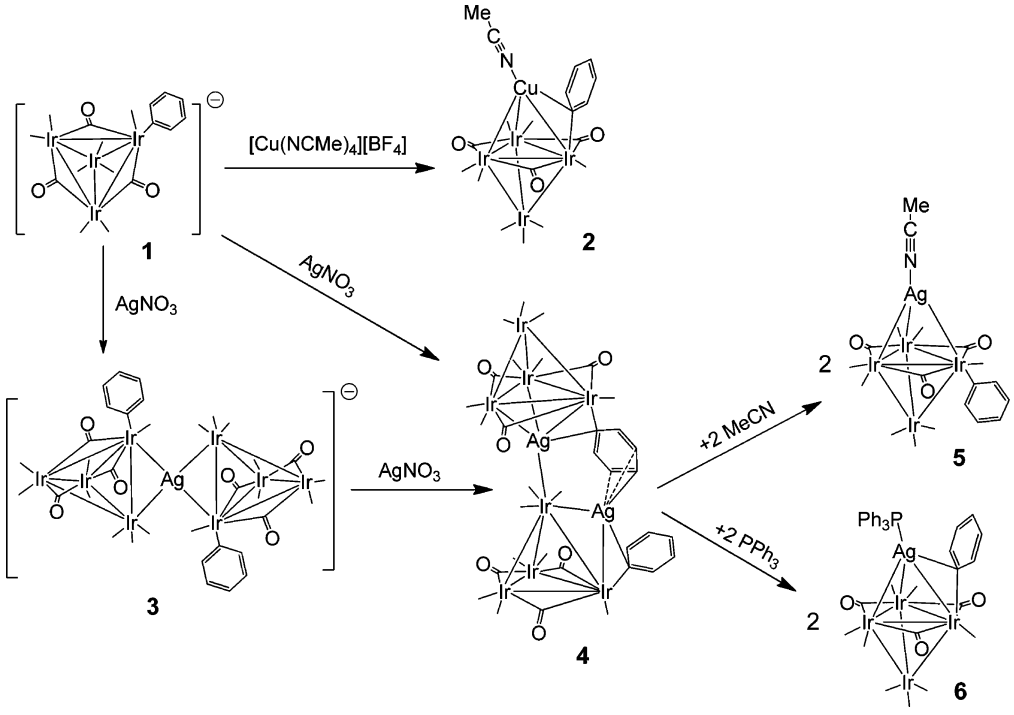

Figure 10 shows the QTAIM analyzed bond paths and lists the selected electron densities at the BCPs and AIM charges of metal atoms in the optimized structure of **4** on the basis of the wave function obtained from the DFT calculation. The electron densities at the BCPs in the C1−Ag1 and C1−Ir4 bonds are 0.035 and 0.122 e/bohr^3, respectively. Such electron densities indicate that the bond strength between C1 and Ag1 is approximately 30% of the strength of the bond between C1 and Ir4. The electron densities at the BCPs in the C2−Ag2, C3−Ag2, and C3−Ir8 bonds are 0.052, 0.035, and 0.121 e/bohr^3, respectively. Such electron densities are very close to the electron densities at the BCPs of the C1−Cu and C1−Ir2 bonds in **2** and confirm that the phenyl groups are asymmetric semibridging ligands between Ag and Ir atoms. The calculated QTAIM charges of C1, C2, C3, Ag1, Ag2, Ir4, and Ir8 are −0.182, −0.076, −0.216, +0.284, +0.404, +0.440, and +0.471, respectively, which also indicate significant electron donation from the Ag and Ir atoms to the semibridging phenyl carbon. In addition, the calculated Wiberg bond indices for C1−Ag2, C2−Ag2, and C3−Ag2 are 0.07,

dx.doi.org/10.1021/om400133w | *Organometallics* 2013, 32, 2416−2426

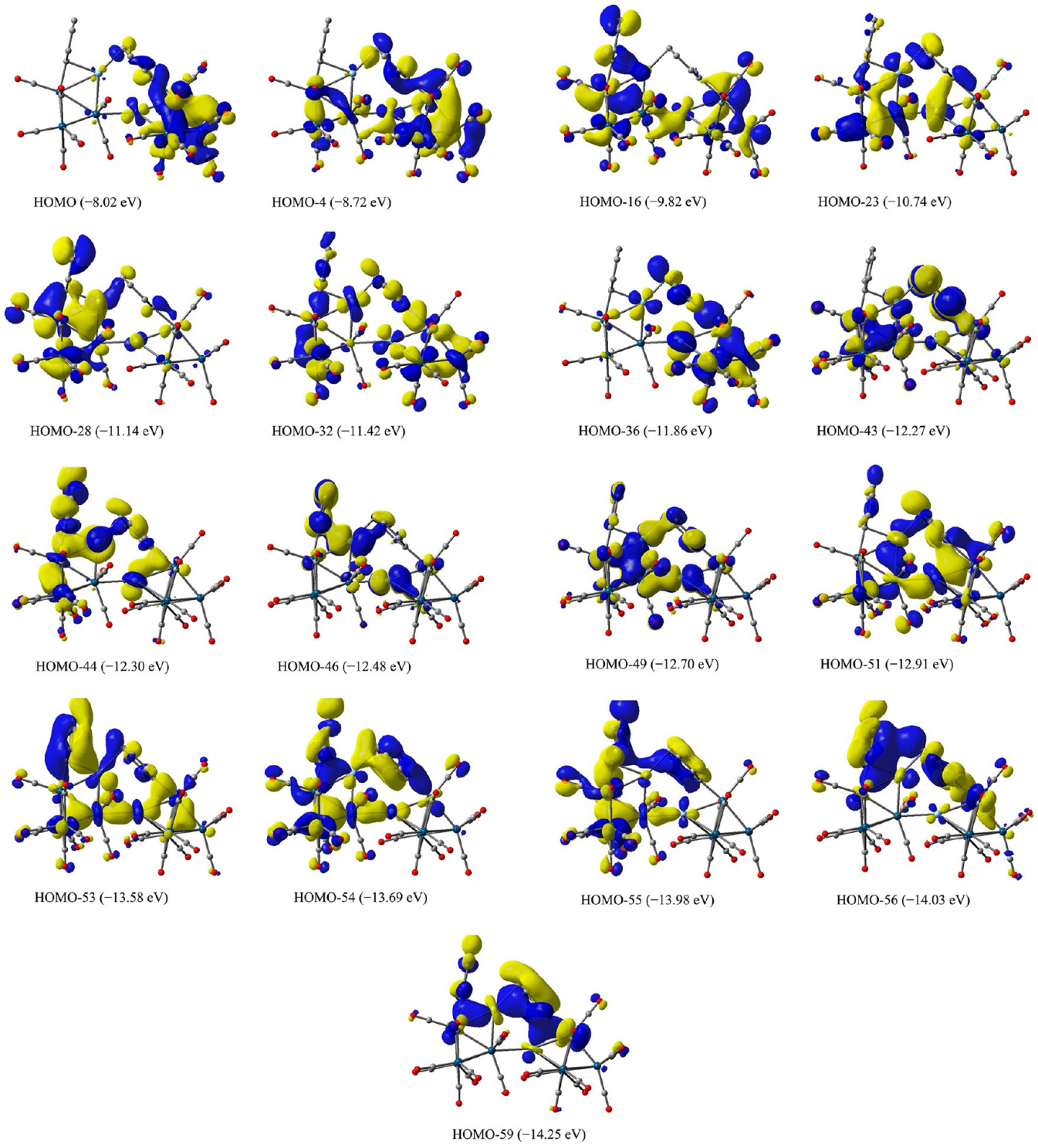

Figure 11. Selected molecular orbitals for **4** showing metal−phenyl ring interactions and calculated energy values.

0.08, and 0.11, respectively. The Wiberg indices for the C1−Ir4 and C3−Ir8 bonds are considerably larger, 0.434 and 0.442, respectively, as expected. Similarly, the corresponding Mayer bond indices are 0.09, 0.25, and 0.28 for C1−Ag2, C2−Ag2, and C3−Ag2 and 0.88 and 0.73 for C1−Ir4 and C3−Ir8, respectively (see Table 1). These bond indices further confirm that the phenyl ligands are asymmetrically semibridging between the Ag and Ir atoms.

Selected MOs obtained from a geometry-optimized DFT calculation of compound **4** that illustrate the bonding interactions between the phenyl rings and the metal atoms implied in the foregoing discussion are shown in Figure 11. The DFT calculated energy gap between the HOMO and the LUMO of **4** is 6.94 eV. The σ-bonding interactions between the p orbitals of the semibridging phenyl carbon atoms and the iridium atoms to which they are primarily coordinated are shown in HOMO-32 and -36. Donation from π orbitals on the ipso-carbon atoms of the rings to the silver atoms are shown in HOMO-16, -23, -56, and -59. Most importantly, there is evidence for significant orbital interactions between the para ring carbon atom of the triply bridging phenyl ring to the neighboring silver atom Ag2 in

dx.doi.org/10.1021/om400133w | *Organometallics* 2013, 32, 2416−2426

HOMO-28, -44, -49, -51, -54, -55, and -59. HOMO-43 shows a strong π-back-bonding interaction between the ipso carbon of the triply bridging phenyl ring and Ir4. HOMO-46 and -49 show weak π-back-bonding interactions between the para ring carbon atom of the triply bridging phenyl ring to the neighboring silver atom Ag2. We were unable to find any significant π-back-bonding interactions between the silver atom Ag1 and C1. On the basis of the above analysis, we conclude that the triply bridging phenyl ligand serves formally as a three-electron donor.

SUMMARY AND CONCLUSIONS

In this work, we have expanded our syntheses of mixed-metal iridium cluster complexes using the phenyl-containing iridium carbonyl anion **1** from gold[9,10] to copper and silver (see Scheme 2). In three of the new compounds, **2**, **4**, and **6**, the phenyl ligand has adopted a semibridging coordination to the heterometal atom. A molecular orbital analysis of **2** revealed the existence of small but significant orbital interactions between the filled π orbitals of the semibridging phenyl ring and the heterometal atom but no significant π back-bonding between the metal atoms and the empty ring π orbitals. In compound **4**, there is a second and rare triply bridging phenyl ligand that formally serves as a three-electron donor. Molecular orbital analyses show that in addition to the usual σ donation of the phenyl rings to the metal atoms, the filled π orbitals of the ring do engage in some π donation to the metal atoms, but there seems to be very little π back-bonding from the metal atoms into the π^* orbitals of the phenyl rings in **4**.

ASSOCIATED CONTENT

Supporting Information

CIF files, text, and tables giving crystallographic data for compounds **2**–**6**, details of the computations, and Cartesian coordinates. This material is available free of charge via the Internet at http://pubs.acs.org.

AUTHOR INFORMATION

Corresponding Author

*E-mail: Adamsrd@mailbox.sc.edu (R.D.A.); xyang@iccas.ac.cn (X.Y.).

Notes

The authors declare no competing financial interest.

ACKNOWLEDGMENTS

This research was supported by the National Science Foundation (Grant CHE-1111496). X.Y. acknowledges financial support by the Molecular Graphics and Computation Facility (Dr. Kathleen A. Durkin, Director) in the College of Chemistry at University of California, Berkeley, and the National Science Foundation (Grant CHE-0840505).

REFERENCES

(1) (a) van Koten, G. *J. Organomet. Chem.* **1990**, *400*, 283–301. (b) Stollenz, M.; Meyer, F. *Organometallics* **2012**, *31*, 7708–7727. (c) Meyer, E. M.; Gambarotta, S.; Floriani, C.; Chiesi-Villa, A.; Guastini, C. *Organometallics* **1989**, *8*, 1067–1079.

(2) (a) Bradford, C. W.; Nyholm, R. S.; Gainsford, G. J.; Guss, J. M.; Ireland, P. R.; Mason, R. *J. Chem. Soc., Chem. Commun.* **1972**, 87–89. (b) Arce, A. J.; Arrojo, P.; Deeming, A. J.; De Sanctis, Y. *J. Chem. Soc., Chem. Commun.* **1991**, 1491–1492. (c) Adams, R. D.; Captain, B.; Zhu, L. *Inorg. Chem.* **2007**, *46*, 4605–4611. (d) Deng, M.; Leong, W. K. *Dalton Trans.* **2002**, 1020–1023. (e) Adams, R. D.; Pearl, W. C., Jr. *J. Organomet. Chem.* **2011**, *696*, 1198–1210. (f) Garcia, M. E.; Ramos, A.; Ruiz, M. A.; Lanfranchi, M.; Marchio, L. *Organometallics* **2007**, *26*, 6197–6212. (g) Briard, P.; Cabeza, J. A.; Llamazares, A.; Ouahab, L.; Riera, V. *Organometallics* **1993**, *12*, 1006–1008. (h) Cabeza, J. A.; Franco, R. J.; Llamazares, A.; Riera, V. *Organometallics* **1994**, *13*, 55–59.

(3) (a) Moret, M.-E.; Chen, P. *Organometallics* **2008**, *27*, 4903–4916. (b) Moret, M.-E.; Chen, P. *J. Am. Chem. Soc.* **2009**, *131*, 5675–5690. (c) Fernandez, E. J.; Laguna, A.; Lopez-de-Luzuriaga, J. M.; Monge, M.; Montiel, M.; Olmos, M. E.; Rodriguez-Castillo, M. *Organometallics* **2006**, *25*, 3639–3646.

(4) (a) Cotton, F. A. *Prog. Inorg. Chem.* **1976**, *21*, 1–28. (b) Colton, R.; McCormick, M. G. *Coord. Chem. Rev.* **1980**, *31*, 1–52.

(5) (a) Adams, R. D.; Kan, Y.; Zhang, Q. *Organometallics* **2011**, *30*, 328–333. (b) Farrugia, L. J.; Miles, A. D.; Stone, F. G. A. *J. Chem. Soc., Dalton Trans.* **1984**, 2415–2422. (c) Hoferkamp, L. A.; Rheinwald, G.; Stoeckli-Evans, H.; Suss-Fink, G. *Organometallics* **1996**, *15*, 704–712. (d) Shima, T.; Suzuki, H. *Organometallics* **2005**, *24*, 1703–1708. (e) Akita, M.; Hua, R.; Oku, T.; Tanaka, M.; Moro-oka, Y. *Organometallics* **1996**, *15*, 4162–4177. (f) Alvarez, M. A.; Garcia, M. E.; Martinez, M. E.; Ramos, A.; Ruiz, M. A. *Organometallics* **2009**, *28*, 6293–6307.

(6) Al-Mandhary Muna, R. A.; Lewis, J.; Raithby, P. R. *J. Organomet. Chem.* **1997**, *530*, 247–250.

(7) Adams, R. D.; Chen, M. *Organometallics* **2011**, *30*, 5867–5872.

(8) Adams, R. D.; Chen, M. *Organometallics* **2012**, *31*, 445–450.

(9) Adams, R. D.; Chen, M.; Yang, X. *Organometallics* **2012**, *31*, 3588–3598.

(10) Adams, R. D.; Chen, M. *Organometallics* **2012**, *31*, 6457–6465.

(11) (a) Crabtree, R. H. *Top. Organomet. Chem.* **2011**, *34*, 1–10. (b) Montserrat, D.; Oscar, P.; Claver, C. *Topics Organomet. Chem.* **2011**, *34*, 11–29. (c) Woodmansee, D. H.; Pfaltz, A. *Top. Organomet. Chem.* **2011**, *34*, 31–76. (d) Choi, J.; Goldman, A. S. *Topics Organomet. Chem.* **2011**, *34*, 139–167. (e) Hartwig, J. F.; Pouy, M. J. *Top. Organomet. Chem.* **2011**, *34*, 169–208. (f) Choi, J.; MacArthur, A. H. R.; Brookhart, M.; Goldman, A. S. *Chem. Rev.* **2011**, *111*, 1761–1779.

(12) (a) Lu, J.; Pedro Serna, P.; Aydin, C.; Browning, N. D.; Gates, B. C. *J. Am. Chem. Soc.* **2011**, *133*, 16186–16195. (b) Gates, B. C. *Chem. Rev.* **1995**, *95*, 511–522. (c) Bayram, E.; Zahmakiran, M.; Ozkar, S.; Finke, R. G. *Langmuir* **2010**, *26*, 12455–12464. (d) Uzun, A.; Dixon, D. A.; Gates, B. C. *ChemCatChem* **2011**, *3*, 95–107. (e) Kulkarni, A.; Lobo-Lapidus, R.; Gates, B. *Chem. Commun.* **2010**, *46*, 5997–6015. (f) Fonseca, G. S.; Umpierre, A. P.; Fichtner, P. F. P.; Teixeira, S. R.; Dupont, J. *Chem. Eur. J.* **2003**, *9*, 3263–3269. (g) Gates, B. C. In *Catalysis by Di- and Polynuclear Metal Complexes*; Adams, R. D., Cotton, F. A., Eds.; Wiley-VCH: New York, 1998; Chapter 14.

(13) (a) Oliver-Meseguer, J.; Cabrero-Antonino, J. R.; Dominquez, I.; Leyva-Perea, A.; Corma, A. *Science* **2012**, *338*, 1452–1455. (b) Haruta, M. *Gold Bull.* **2004**, *37*, 27–36. (c) Haruta, M. *Catal. Today* **1997**, *36*, 153–166. (d) Haruta, M.; Date, M. *Appl. Catal. A: Gen.* **2001**, *222*, 427–437. (e) Hashmi, A. S. K.; Hutchings, G. J. *Angew. Chem., Int. Ed.* **2006**, *45*, 7896–7936. (f) Della Pina, C.; Falletta, E.; Prati, L.; Rossi, M. *Chem. Soc. Rev.* **2008**, *37*, 2077–2095. (g) Lee, S.; Molina, L. M.; Lopez, M. J.; Alonso, J. A.; Hammer, B.; Lee, B.; Seifert, S.; Winans, R. E.; Elam, J. W.; Pellin, M. J.; Vajda, S. *Angew. Chem., Int. Ed.* **2009**, *48*, 1467–1471. (h) Bravo-Suarez, J. J.; Lu, J.; Fujitani, T.; Oyama, S. T. *J. Catal.* **2008**, *255*, 114–126. (i) Herzing, A. A.; Kiely, C. J.; Carley, A. F.; Landon, P.; Hutchings, G. J. *Science* **2008**, *321*, 1331–1335. (j) Miedziak, P.; Sankar, M.; Dimitratos, M.; Lopez-Sanchez, J. A.; Carley, A. F.; Knight, D. W.; Taylor, S. H.; Kiely, C. J.; Hutchings, G. J. *Catal. Today* **2011**, *164*, 315–319.

(14) (a) Zhang, Y.; Cui, X.; Shi, F.; Deng, Y. *Chem. Rev.* **2012**, *112*, 2467–2505. (b) Hutchings, G. J. *Chem. Commun.* **2008**, 1148–1164. (c) Lopez-Sanchez, J. A.; Dimitratos, N.; Glanvilla, N.; Kesavan, L.; Hammond, C.; Edwards, J. K.; Carley, A. F.; Kiely, C. J.; Hutchings, G. J. *Appl. Catal. A: Gen.* **2011**, *391*, 400–406. (d) Enache, D. I.; Edwards, J. K.; Landon, P.; Solsona-Espriu, B.; Carley, A. F.; Herzing, A. A.; Watanabe, M.; Kiely, C. J.; Knight, D. W.; Hutchings, G. J. *Science* **2006**, *311*, 362–365. (e) Ortiz-Soto, L. B.; Alexeev, O. S.; Amiridis, M. D. *Langmuir* **2006**, *22*, 3112–3117. (f) Evans, J.; Gao, J. *J. Chem. Soc., Chem. Commun.* **1985**, 39–40. (g) Li, Y.; Pan, W.-X.; Wong, W.-T. *J. Cluster Sci.* **2002**, *13*, 223–233.

(15) Sabater, S.; Mata, J. A.; Peris, E. *Chem. Eur. J.* **2012**, *18*, 6380−6385.
(16) (a) Sculfort, S.; Braunstein, P. *Chem. Soc. Rev.* **2011**, *40*, 2741−2760. (b) Salter, I. D. *Adv. Organomet. Chem.* **1989**, *29*, 249−343. (c) Salter, I. D. In *Comprehensive Organometallic Chemistry II*; Abel, E. W., Stone, F. G. A., Wilkinson, G., Eds.; Pergamon: Oxford, U.K., 1995; Vol. *10*, Chapter 5, pp 255−322.
(17) (a) Mamontov, G. V.; Magaev, O. V.; Knyazev, A. S.; Vodyankina, O. V. *Catal. Today* **2013**, *203*, 122−126. (b) Yamamoto, R.; Sawayama, Y.; Shibahara, H.; Ichihashi, Y.; Nishiyama, S.; Tsuruya, S. *J. Catal.* **2005**, *234*, 308−317.
(18) *SAINT+, version 6.2a*, Bruker Analytical X-ray Systems, Inc., Madison, WI, 2001.
(19) Sheldrick, G. M. *SHELXTL, version 6.1*; Bruker Analytical X-ray Systems, Inc., Madison, WI, 1997.
(20) Frisch, M. J.; Trucks, G. W.; Schlegel, H. B.; Scuseria, G. E.; Robb, M. A.; Cheeseman, J. R.; Scalmani, G.; Barone, V.; Mennucci, B.; Petersson, G. A.; Nakatsuji, H.; Caricato, M.; Li, X.; Hratchian, H. P.; Izmaylov, A. F.; Bloino, J.; Zheng, G.; Sonnenberg, J. L.; Hada, M.; Ehara, M.; Toyota, K.; Fukuda, R.; Hasegawa, J.; Ishida, M.; Nakajima, T.; Honda, Y.; Kitao, O.; Nakai, H.; Vreven, T.; Montgomery, J. A., Jr.; Peralta, J. E.; Ogliaro, F.; Bearpark, M.; Heyd, J. J.; Brothers, E.; Kudin, K. N.; Staroverov, V. N.; Kobayashi, R.; Normand, J.; Raghavachari, K.; Rendell, A.; Burant, J. C.; Iyengar, S. S.; Tomasi, J.; Cossi, M.; Rega, N.; Millam, N. J.; Klene, M.; Knox, J. E.; Cross, J. B.; Bakken, V.; Adamo, C.; Jaramillo, J.; Gomperts, R.; Stratmann, R. E.; Yazyev, O.; Austin, A. J.; Cammi, R.; Pomelli, C.; Ochterski, J. W.; Martin, R. L.; Morokuma, K.; Zakrzewski, V. G.; Voth, G. A.; Salvador, P.; Dannenberg, J. J.; Dapprich, S.; Daniels, A. D.; Farkas, Ö.; Foresman, J. B.; Ortiz, J. V.; Cioslowski, J.; Fox, D. J. *Gaussian 09, Revision C.01, suite of programs for ab initio calculation*; Gaussian, Inc., Wallingford, CT, 2010.
(21) Chai, J. -D.; Head-Gordon, M. *Phys. Chem. Chem. Phys.* **2008**, *10*, 6615−6620.
(22) (a) Figgen, D.; Rauhut, G.; Dolg, M.; Stoll, H. *Chem. Phys.* **2005**, *311*, 227−244. (b) Peterson, K. A.; Puzzarini, C. *Theor. Chem. Acc.* **2005**, *114*, 283−296.
(23) Figgen, D.; Peterson, K. A.; Dolg, M.; Stoll, H. *J. Chem. Phys.* **2009**, *130*, 164108-1−164108-13.
(24) Dunning, T. H., Jr. *J. Chem. Phys.* **1989**, *90*, 1007−1023.
(25) (a) Jensen, F. *Chem. Theory Comput.* **2010**, *6*, 2726−2735. (b) Thanthiriwatte, K. S.; Hohenstein, E. G.; Burns, L. A.; Sherrill, C. D. *J. Chem. Theory Comput.* **2011**, *7*, 88−96.
(26) *ADF2012*; SCM Theoretical Chemistry, Vrije Universiteit, Amsterdam, The Netherlands (http://www.scm.com).
(27) (a) Tao, J.; Perdew, J. P.; Staroverov, V. N.; Scuseria, G. E. *Phys. Rev. Lett.* **2003**, *91*, 146401−146404. (b) Staroverov, V. N.; Scuseria, G. E.; Tao, J.; Perdew, J. P. *J. Chem. Phys.* **2003**, *119*, 12129.
(28) (a) Bader, R. F. W. *Atoms in Molecules: A Quantum Theory*; Clarendon: Oxford, U.K., 1990. (b) Cortés-Guzmán, F.; Bader, R. F. W. *Coord. Chem. Rev.* **2005**, *249*, 643.
(29) Keith, T. A. *AIMAll, Version 12.11.09*; TK Gristmill Software, Overland Park, KS, 2012 (aim.tkgristmill.com).
(30) Wiberg, K. B. *Tetrahedron* **1968**, *24*, 1083−1096.
(31) Glendening, E. D.; Badenhoop, J. K.; Reed, A. E.; Carpenter, J. E.; Bohmann, J. A.; Morales, C. M.; Weinhold, F. *NBO 5.0*; Theoretical Chemistry Institute, University of Wisconsin, Madison, WI, 2001.
(32) Mayer, I. *J. Comput. Chem.* **2007**, *28*, 204−221.
(33) Olmstead, M. M.; Power, P. P. *J. Am. Chem. Soc.* **1990**, *112*, 8008−8014.
(34) Gambarotta, S.; Strobgo, S.; Floriani, C.; Chiesi-Villa, A.; Guastini, C. *Organometallics* **1984**, *3*, 1444−1445.
(35) Della Pergola, R.; Garlaschelli, L.; Demartin, F.; Manassero, M.; Masciocchi, N. *J. Organomet. Chem.* **1992**, *436*, 241−253.
(36) Fajardo, M.; Gomez-Sal, M. P.; Holden, H. D.; Johnson, B. F. G.; Lewis, J.; McQueen, R. C. S.; Raithby, P. R. *J. Organomet. Chem.* **1984**, *267*, C25−C28.
(37) Heaton, B. T.; Strona, L.; Martinengo, S.; Strumolo, D.; Albano, V. G.; Braga, D. *J. Chem. Soc., Dalton Trans.* **1983**, 2175−2182.